NANO LETTERS
Cite This: Nano Lett. 2018, 18, 4704−4709
Letter
pubs.acs.org/NanoLett

Modification of the Potential Landscape of Molecular Rotors on Au(111) by the Presence of an STM Tip

Hong-Liang Lu,[†] Yun Cao,[†] Jing Qi,[†] Anne Bakker,[‡] Cristian A. Strassert,[‡] Xiao Lin,[†] Karl-Heinz Ernst,[§] Shixuan Du,*[,†] Harald Fuchs,[‡] and Hong-Jun Gao*[,†]

[†]Institute of Physics & University of Chinese Academy of Sciences, Chinese Academy of Sciences, Beijing 100190, P. R. China
[‡]Physikalisches Institut, Westfälische Wilhelms-Universität & Center for Nanotechnology (CeNTech), Wilhelm-Klemm-Straße 10, 48149 Münster, Germany
[§]Nanoscale Materials Science, Empa, Swiss Federal Laboratories for Materials Testing and Research, Überlandstrasse 129, CH-8600 Dübendorf, Switzerland

Supporting Information

ABSTRACT: Molecular rotors on solid surfaces are fundamental components of molecular machines. No matter whether the rotation is activated by heat, electric field or light, it is determined by the intrinsic rotational potential landscape. Therefore, tuning the potential landscape is of great importance for future applications of controlled molecular rotors. Here, using scanning tunneling microscopy (STM), we demonstrate that both tip−molecule distance and sample bias can modify the rotational potential of molecular rotors. We achieve the potential energy difference variations of ∼0.3 meV/pm and ∼18 meV/V between two configurations of a molecular rotor, a tetra-*tert*-butyl nickel phthalocyanine molecule on Au(111) substrate. Further analysis indicates that the mechanism of modifying the rotational potential is a combination of the van der Waals interaction and the interaction between the molecular dipole and an electric field. This work provides insight into the methods used to modify the effective rotational potential energy of molecular rotors.

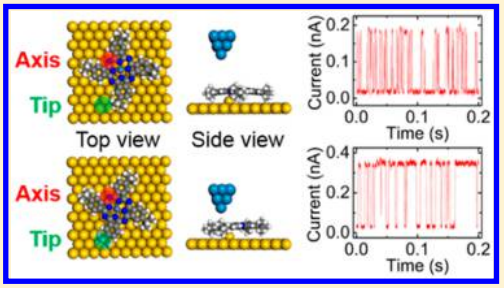

Molecular machines are ubiquitous in nature and play essential roles in many biological processes, such as cellular transport, muscle contraction and genetic transcription.[1−3] Chemists have synthesized molecular machines, including four-wheeled molecular nanocars,[4,5] molecular motors,[6−10] and molecular gears.[11,12] Although different in structure, function, and working principle from natural motor proteins, these can constitute a basis for future nanotechnology. As key components of molecular machines, molecular rotors attracted great attention,[13−20] because their design and control are fundamental for the development of more complicated molecular actuators. So far, controlling the "on" and "off" states of molecular rotors was realized by charge state,[21] selection of anchoring site,[22] and interaction between rotors and surrounding molecules.[13,23] However, controlling the rotors' residence time distribution in different rotational configurations is still missing.

Compared with processes in solutions, molecular rotors mounted on solid surfaces have many advantages. They are easily accessible by an external field and addressable by surface analysis techniques.[15] Scanning tunneling microscopy (STM), as constituting tool of nanotechnology, has been used for imaging molecular rotors with high spatial resolution[13,15,24] and studying the dynamics of molecules induced by inelastic electron tunneling. Although limited in time resolution, it has the capability to study dynamics,[14,22,25,26] including molecular rotors on solid surfaces. Besides characterization of molecular rotors, STM has been demonstrated to be a unique instrument in manipulation of molecular rotors using various schemes involving STM tips.[9,18,19,27,28] However, the van der Waals interaction between STM tip and molecular rotors and how their rotational behavior is influenced by this interaction are rarely studied experimentally. Gehrig et al. showed recently that thermal activation barriers for rotation of a dialkylthioether depend strongly on the STM tip position above the molecule.[26]

Here, we achieve the tip-influenced rotational switch of single tetra-*tert*-butyl nickel phthalocyanine ((*t*-Bu)$_4$-NiPc) molecules on Au(111). It is found that the residence time distribution of a molecule on two neighboring rotational configurations (UT-state and N-state), which is determined by the rotational potential landscape, can be tuned by the tip−molecule interaction. We demonstrate that the variations of the potential energy difference are ∼0.3 meV/pm when the tip−sample distance changes within 100 pm, and ∼18 meV/V when a sample bias changes from −1 to −0.2 V, respectively. Furthermore, by employing the Arrhenius equation, we find that the transition barrier from UT-state to N-state increases 24 meV while the tip height decreases 100 pm. Our findings

Received: March 14, 2018
Revised: June 21, 2018
Published: July 2, 2018

DOI: 10.1021/acs.nanolett.8b01019
Nano Lett. 2018, 18, 4704−4709

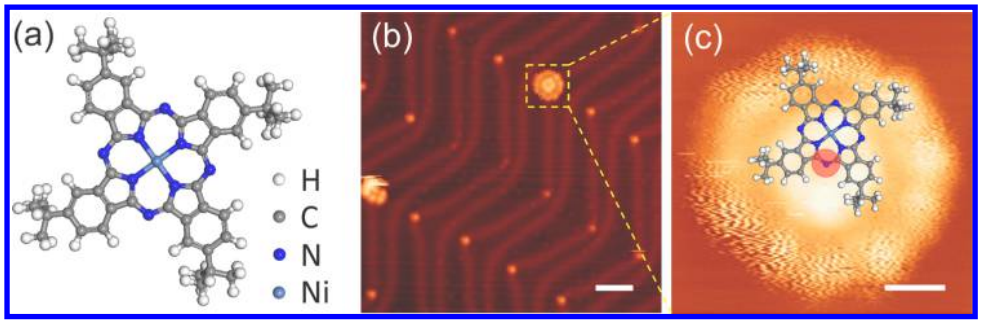

Figure 1. Molecular structure and STM images. (a) Molecular structure of $(t\text{-Bu})_4$-NiPc. (b) Large area STM image showing a Au(111) surface with herringbone reconstruction and a rotating $(t\text{-Bu})_4$-NiPc molecule at an elbow position. (c) Close-up STM image of the molecule in part b, overlaid with a molecular model. The rotation axis (red spot) is located at a nitrogen atom and the protrusions are due to butyl groups. Scale bars are 5 nm in part b and 1 nm in part c. Images are obtained at $V_{Sample} = -1$ V, $I = 50$ pA, and $T = 78$ K.

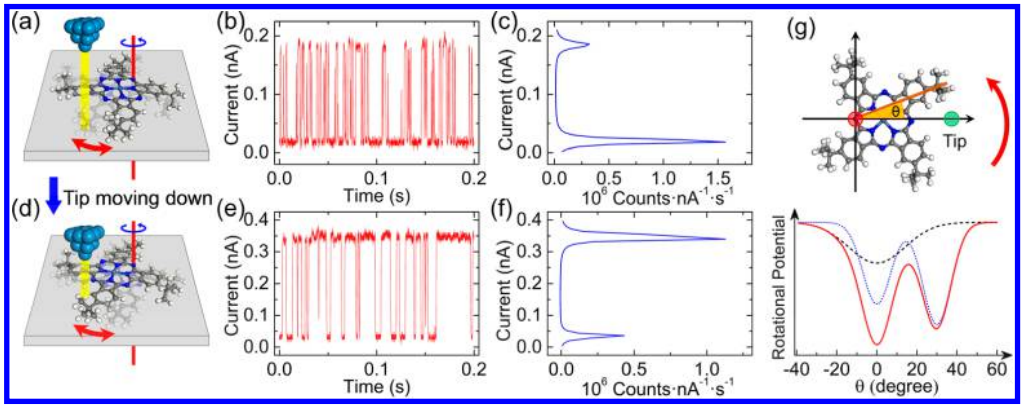

Figure 2. Effect of STM tip height on the occupation probability of two neighboring configurations of a molecular rotor. (a) Sketch of the dominant adsorption configuration of $(t\text{-Bu})_4$-NiPc on Au(111) when the tip is far away; the solid model shows the dominant configuration with a butyl group in the second nearest position to the tip (denoted as neighbor configuration); the transparent model shows a metastable configuration with a butyl group in the nearest position to the tip (denoted as under-tip configuration, abbreviated as UT). (b and c) Corresponding $I-t$ spectrum and current distribution. (d) Sketch of adsorption configuration of $(t\text{-Bu})_4$-NiPc after the tip approaches the sample surface. The UT-configuration becomes dominant (solid model), and the neighbor configuration becomes metastable (transparent model). (e and f) are the $I-t$ spectrum and current distribution in the case of part d. (g) Schematic representation of the rotational potential energy around UT- and N-configurations consisting of the native potential well without tip molecule interaction (blue dotted line); the tip-induced potential well (black dashed line); the potential landscape with added contributions of the native and tip-induced potentials (red solid line). The molecular model on top defines the geometric relationship of $(t\text{-Bu})_4$-NiPc, rotation axis (red dot) and tip position (green dot). $V_{Sample} = -1$ V and the feedback loop is open. The time resolutions in parts b and e are 40 μs. The bin sizes are 0.004 nA in part c and 0.008 nA in part f.

provide useful information about the influence of external forces on the rotational potential landscape of molecular rotors on a solid surface.

The $(t\text{-Bu})_4$-NiPc molecule studied in this work (see Figure 1a for the structure) was synthesized and purified following the procedure by Hanack et al.[29−31] When the molecule is pinned by defects on the Au(111) surface, it shows 4 bright lobes (Figure S1), which are attributed to its $(t\text{-Bu})_4$-groups, quite similar to the Zn analogue of the same ligand.[23,32] However, it is more common that the single molecule appears in a round shape with several bright protrusions (Figure 1b and 1c), a feature that comes from the thermally activated rotation on the Au(111) surface at 78 K, as also observed for $(t\text{-Bu})_4$-ZnPc on Au(111).[14] The molecule is hopping between several metastable configurations around an off-centered axis. This axis is formed by a chemical bond between one of the imine nitrogen atoms and a gold atom on the elbow position of the reconstructed Au(111) surface.[14] Therefore, the axis is fixed on the surface and the hopping results in a random rotational motion around this axis. There are two circles of protrusions around the rotating axis. The inner and outer protrusions are representing the $(t\text{-Bu})_4$-groups near and far from the fixed N atom (as shown in the molecular model in Figure 1c), respectively.[14]

Figure 2 shows the effect of STM tip height on the occupation probability of two neighboring configurations of the molecular rotor. When an STM tip in tunneling state was positioned over the outer circle of a rotating molecule, as shown schematically in Figure 2a,d (and also shown in Figure 3a and the inset of Figure 4a), the feedback loop was turned off and the $I-t$ spectra were measured. The typical $I-t$ spectra show two distinct current levels (Figure 2b), indicating that the molecule is rotationally hopping or switching randomly between two configurations[21] but not necessarily performing a 360 deg rotation. The high current level could be assigned to the molecular configuration with one butyl group in the nearest position to the tip (denoted as under-tip configuration hereafter, abbreviated as "UT"), while the low current level corresponds to another configuration with the butyl group in the second nearest position to the tip (denoted as neighbor configuration, abbreviated as "N").[8,25] Interestingly, when the tip moves closer to the molecule in the vertical direction, as schematically shown in Figure 2d, the occupation probability of each configuration changes. Specifically, the dominant

DOI: 10.1021/acs.nanolett.8b01019
Nano Lett. 2018, 18, 4704−4709

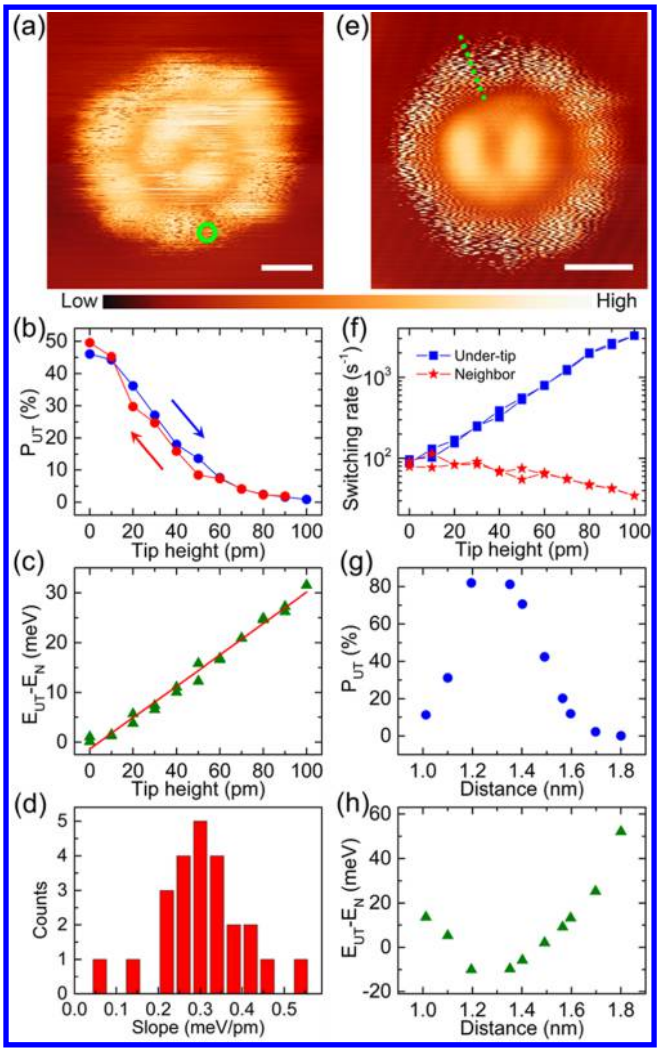

Figure 3. Modifying the potential energy of molecular rotors by varying the tip−molecule distance. (a) STM image of a rotating molecule for I−t spectra measurement at various tip heights. The green circle indicates the tip position in this experiment. (b) Tip height dependent occupation probability for the under-tip (UT) configuration obtained by calculating the percentage of high-current level in the I−t spectra. The measurement sequence is from 0 pm (close to the molecule) to 100 pm (far away from the molecule) and then backward to 0 pm with steps of 10 pm, as indicated by the blue and red arrows. A tip height of 0 pm corresponds to a tunneling current of 1.3 nA at a sample bias of −1 V. (c) Corresponding potential energy difference between the under-tip and neighbor configurations ($E_{UT} - E_N$). The red line is a linear fit. (d) Distribution histogram for the slope of E_{UT}-E_N vs tip height as plotted in part c in repeated measurements on different molecules and/or different positions. (e) Constant current STM image of a rotating molecule. The blurring features are due to rapid fluctuations of the molecule. A series of I−t spectra was recorded on the molecule. Each I−t spectrum was acquired at a fixed position on the green line, while the tip height was kept constant. (f) Switching rate for the under-tip and neighbor configurations, obtained by fitting the integrated resident time distribution of I−t spectra at each tip height (see Figure S2 for details). (g and h) under-tip probability and $E_{UT} - E_N$ for different lateral tip−axis distances with constant tip height. STM parameters for topography images: V_s = −1 V and I_t = 50 pA. For I−t spectra measurement, the feedback loop is open and the sample bias is −1 V. Scale bars are 1 nm. Lines in parts b and f are guides for the eyes.

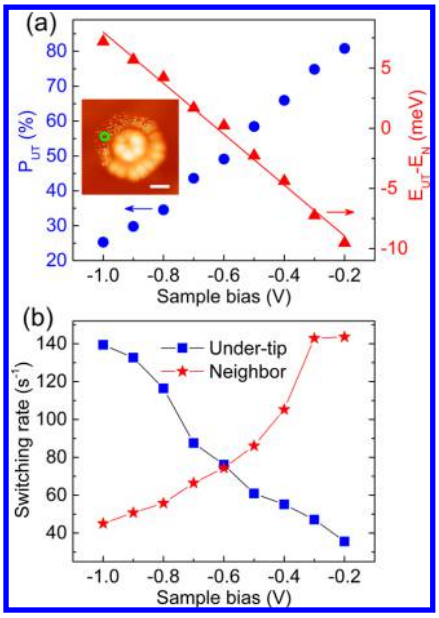

Figure 4. Variation of occupation probability, potential energy and switching rate with sample bias. (a) Sample bias dependent occupation probability of the under-tip state (P_{UT}, blue filled circles) and potential difference between under-tip and neighbor configurations ($E_{UT} - E_N$, red filled triangles). The red line is a linear fit. The inset shows the STM image of a rotating molecule and the green circle indicates the tip position where the I−t spectra were obtained. (b) Switching rate for under-tip and neighbor configurations at different sample bias. Lines are used to guide the eyes. The tip position is fixed and feedback loop is open during the variation of sample bias. Data shown here are obtained by analyzing I−t spectra at each sample bias. For STM image: V_s = −1 V and I_t = 50 pA. Scale bar is 1 nm.

configuration changes from N-state to UT-state, as revealed by the I−t spectra (Figure 2, parts b and e) and occupation probability (Figure 2, parts c and f). Since the occupation probability is determined by the potential energy of each configuration, the change of dominant configuration at different tip−molecule distances reveals that the rotational potential energy of a molecular rotor varies with tip−molecule distance. The potential well variation with tip height is schematically shown in Figure 2g. It should be mentioned that the potential energy discussed here is only an effective one explored by the random rotation of the molecule. The real potential energy surface for describing the molecular rotation is much more complicated in view of large number of degrees of freedom of the molecule.

In a previous work, the $(t\text{-Bu})_4$-ZnPc molecules did not rotate at 5 K but rotated at 78 K at the same tunneling current.[14,23] $(t\text{-Bu})_4$-NiPc is very similar to $(t\text{-Bu})_4$-ZnPc. Therefore, we think that the rotation of $(t\text{-Bu})_4$-NiPc is mainly thermally activated at 78 K and the tunneling current has less effect on the potential landscape. Figure 3 shows the quantitative results of tip−molecule distance effects on the molecular rotational potential energy. The topography image of a rotating molecule under investigation is shown in Figure 3a. The green circle indicates where the tip is located during the measurement, in which the tip moves only in vertical direction. We set the tip at different heights with steps of 10 pm each and measure I−t spectra at each point. The resulting UT-state probability (P_{UT}) vs tip height is demonstrated in Figure 3b. We can see that, when the tip height varies from 100

DOI: 10.1021/acs.nanolett.8b01019
Nano Lett. 2018, 18, 4704−4709

to 0 pm (here 0 pm means the tip is close to the molecule and 100 pm means the tip is far away), the UT-state probability changes from almost zero to ~50%. The molecule rotationally switches between the two configurations randomly, with the occupation probability determined by the tip height. The UT-state probability (P_{UT}), as well as the N-state probability (1-P_{UT}), varies gradually with the tip height. The results of repeated measurements are also shown in Figure 3b by increasing (blue arrow) and decreasing (red arrow) tip height. Both lines almost overlap, indicating good repeatability and reliability of the experimental results. The variation of $I-t$ spectra and the corresponding distribution of currents with tip height for a typical example is shown in the movie in the Supporting Information.

The occupation probability of the UT- and N-states could be considered to follow the Boltzmann distribution,[33] so the energy difference between the two configurations could be derived using the equation: $E_{UT} - E_N = -kT \ln\left(\frac{P_{UT}}{1-P_{UT}}\right)$, where k is the Boltzmann constant, T is temperature in kelvin, and E_{UT} and E_N are the potential energy of the UT- and N-configurations, respectively. The energy difference at each tip height is plotted in Figure 3c. We can see that the potential energy of a molecular rotor in the UT-configuration relative to the N-configuration could be modified in a controllable way. The potential energy variation rate with tip height is 0.32 meV/pm (i.e., the slope of the linear fit in Figure 3c) and a total energy variation is ~31 meV in this experiment. A stronger effect is expected when the tip is moved over a larger range. We then measured the $I-t$ spectra at various tip heights at different sites on the outer circles of rotating molecular rotors, and obtained 24 groups of valid data on four sites of two molecules. All these data show the same tendency that the energy difference $E_{UT} - E_N$ decreases when the tip approaches to the lobe of a molecule. Figure 3d shows the distribution of the potential variation rate derived from these data, which gives an average value of ~0.3 meV/pm. The decrease of $E_{UT} - E_N$ with the decrease of the tip−molecule distance suggests that the interaction between the tip and the molecule is a van der Waals like interaction in the attractive force region (see the Supporting Information for more discussion).

The van der Waals interaction is commonly utilized in atomic or molecular manipulation to facilitate translational motion of atoms or molecules.[34−36] Here, when we bring the STM tip close to a lobe by lowering the tip height, the butyl group of (t-Bu)$_4$-NiPc molecule will be attracted by the tip. This leads to a decreased potential energy of the under-tip conformation and increases the probability of the high-current level in an $I-t$ spectrum. Because of the existence of a rotational axis, i.e. the strong chemical bond between Au adatom and the imine nitrogen,[14] the butyl group is confined in the circle surrounding this axis. The tip height dependent energy variation, with an average value of ~0.3 meV/pm, is of the same order of magnitude as the van der Waals force between a metal tip and organic molecules,[37] which confirms that the attractive interaction observed here is the van der Waals force.

The rotational switching rate could be obtained from $I-t$ spectra by fitting the integrated residence time distribution of the states at high or low current (Figure S2).[21,38] Switching rate here is the probability of transition per unit time and means the statistically averaged inverse lifetime of each level. A typical current dependent switching rate for the transition from neighbor to under-tip configurations is shown in Figure S3. The power law fitting using $R \propto I^n$ gives $n = 0.32$, much smaller than 1, indicating a minor contribution of tunneling electrons to the excitation of the rotation.[39] Figure 3f shows the rotational switching rate at different tip heights. We found that the switching rate for switching from the UT-state to the N-state decreases from ~3.2×10^3 to ~90 s^{-1} when tip is lowered by 100 pm, while the switching rate for the reverse pathway changes from ~35 to ~85 s^{-1}. This implies that the barrier for switching from the UT- to the N-state increases considerably when the tip−molecule distance is decreased. Meanwhile, the barrier decreases slightly for the reverse switching leaving both switching rates almost equal at 0 pm. By employing the Arrhenius equation, the potential barrier variations are estimated to be about +24 and −6 meV for UT- and N-states respectively (for details see Figure S4). This is in agreement with the potential energy variation schematically shown in Figure 2g.

Modifying the potential energy of the UT-state by approaching the tip to the molecule could also be realized by moving the tip laterally while keeping the tip height constant. Figure 3e shows a molecular rotor in such an experiment. Parts g and h of Figure 3 present the UT-state probability and the corresponding potential energy difference between the two states at different tip positions along the green dashed line in Figure 3e. We found that, when the tip approaches the lobe, the UT-state probability increases and its potential energy decreases, vice versa. We repeated this experiment at four sites on two molecules and all the results exhibit the same tendency. The variation of the probability and potential energy with the lateral displacement of the STM tip further demonstrates that increasing the attractive tip−molecule interaction could reduce the potential energy of the under-tip molecular configuration.

In order to further clarify the contribution of the electric field in the rotating behavior of molecular rotors, we measured the $I-t$ spectra at different sample bias and polarity with the tip positioned over the outer circle of a rotating molecule and the tip height kept constant by turning off the feedback. Figure 4a illustrates the UT-state probability P_{UT} at varying negative sample bias. We can see that P_{UT} decreases with increasing bias voltage. In other words, the potential well below the tip becomes shallower with increasing electric field. We also measured the $I-t$ spectra at a positive sample bias for several times, and never observed tunneling current switching, indicating no molecular rotation related to a deeper potential well below the tip. Atoms or molecules adsorbed on metal surfaces could be considered as static and induced dipoles in an electric field.[40−42] It was reported that the static dipole moment of Cs atoms on a GaAs(110) substrate is considered normal to the surface, and application of a positive sample bias will induce segregation of the Cs atoms under the tip, driven by a local potential energy gradient arising from the interaction between the atomic dipole moment and the electric field gradient.[40,41] Besides, iron phthalocyanine (FePc) molecules on Au(111) could be viewed as an electric dipole normal to the sample surface, and an applied electric field was utilized to retard or enhance molecular diffusion by changing the sample bias.[42] Considering the similarity of (t-Bu)$_4$-NiPc and FePc in structure and the experimental results when changing the bias, it is convincing that there is a static dipole moment in (t-Bu)$_4$-NiPc normal to the sample surface. Following a similar mechanism,[40,41] the negative sample bias, generates an electric

DOI: 10.1021/acs.nanolett.8b01019
Nano Lett. 2018, 18, 4704−4709

field antiparallel to the molecular dipole moment. This will raise the potential energy of the UT-configuration. Further increasing the negative bias will increase the under-tip potential energy, which is in agreement with the experimental results (Figure 4a). A positive sample bias will generate an electric field parallel to the molecular dipole moment, and decrease the potential energy of the UT-configuration, resulting in no rotational switching. The potential difference, deduced from the occupation probability using the formula mentioned above, is also plotted in Figure 4a, the slope is ∼21 meV/V. We can see here that, besides changing the tip−molecule distance, varying the sample bias could also be utilized to modify the potential landscape of molecular rotors effectively. We repeated the experiments with varying bias for seven times on five different molecules, and all the results exhibit the same tendency that the high current (UT-state) probability decreases with increasing sample bias. The average slope is ∼18 meV/V. This result demonstrates the validity of the dipole model discussed above and the feasibility of modifying the potential landscape of molecular motors by changing the sample voltage. Comparing the total magnitude of potential energy variation when changing the bias (∼17 meV, Figure 4a) with the total potential energy variation when changing the tip−molecule distance experiments (∼31 meV, Figure 3c), we find that the former one is smaller. Decreasing the tip−molecule distance will lead to a small increase in electric field, and therefore raise the potential energy a little for the UT-state. However, we observe a large potential energy reduction when the tip approaches the molecule. Therefore, the variation of the potential energy in the experiment of varying tip−molecule distance mainly comes from the van der Waals interaction between tip and molecule other than the interaction between the electric field and the molecular dipole.

Figure 4b shows the rotational switching rate for the UT- and N-configurations at different sample bias. With increasing sample bias, the switching rate increases for the UT-state and decreases for the N-state, indicating that the potential barrier for switching from the UT- to the N-configuration decreases and the barrier for the reverse switching increases. The changes in barrier are estimated to be −9.1 and 7.7 meV for the UT- and N-states respectively when the sample bias changes from −0.2 to −1 V (Figure S5). This is consistent with the scenario discussed above that the potential energy of the UT-configuration increases with increasing sample bias, and concurrently the barrier for switching from the UT- to the N-configuration decreases.

It is interesting to compare our work here with some related previous works. Pawlak et al. reported that the directed rotation of a single porphyrin molecule could be induced by an STM tip.[28] Although both their work and ours utilize the attractive force between tip and molecules, the rotation mechanism is different. In their work the directed rotation is induced by deformation of the porphyrin molecule,[28] specifically the distortion of the dicyanophenyl group, in response to a local mechanical force exerted by the tip. However, in our work, the rotation process is thermally driven for $(t\text{-Bu})_4$-NiPc on Au(111). On the other hand, in their work, the molecule is static before and after tip manipulation, while in our work, the dynamic rotating process is studied. Besides this, Stroscio et al. reported that, by tuning the trapping potential of the STM tip, switching of Co atoms between neighboring hcp and fcc sites on a Cu(111) surface could be controlled.[38] Our work here demonstrates a counterpart that rotational switching of single molecular rotors could be influenced in a similar way.

In conclusion, we have demonstrated that the potential energy surface of molecular rotors could be modified precisely and reliably by the presence of an STM tip. Through measuring the $I-t$ spectra on a rotating $(t\text{-Bu})_4$-NiPc molecule on a Au(111) surface using STM, we revealed that the potential energy of the under-tip configuration could be reduced by decreasing the tip−molecule distance due to attractive van der Waals interaction between them. By increasing the negative sample bias, the potential energy of the under-tip state is increased, which can be attributed to an electrostatic interaction between the molecular dipole moment and the applied electric field. Our work provides useful information on the rotational energy landscape of molecular rotors on solid surfaces in the presence of an STM tip, which should be more carefully considered in future STM studies of molecular motors.

Methods. The experiments were performed in a CreaTec low temperature STM system with a base pressure of 1×10^{-10} mbar. The Au(111) surface was cleaned by repeated cycles of Ar^+ ion sputtering and annealing at 500 °C. Then a small quantity of $(t\text{-Bu})_4$-NiPc molecules was deposited on Au(111) surface using a Knudsen-cell evaporator at 300 °C. The sample was kept at room temperature during deposition in the preparation chamber, and then transferred to the STM chamber for measurement at 78 K. STM images were acquired using constant current mode, while current−time ($I-t$) spectra, for measuring the occupation probability of two adjacent rotational configurations, were obtained with the feedback loop open. Both STM topography images and $I-t$ spectra were measured after the system reached thermal equilibrium. Although the data lengths shown in Figure 2, parts b and e, are 0.2 s for clarity, we used data lengths as long as 4 s for the calculation of the occupation probability at each tip height to reduce the random uncertainty induced by short data length. Electrochemically etched W tips were used in all experiments. Drift compensation was activated and calibrated several times to minimize the error induced by thermal drift and creep (see Figure S6 for the drift rate).

■ ASSOCIATED CONTENT

Supporting Information

The Supporting Information is available free of charge on the ACS Publications website at DOI: 10.1021/acs.nanolett.8b01019.

STM images of static $(t\text{-Bu})_4$-NiPc molecules, typical integrated residence time distributions for under-tip and neighbor states, switching rate from neighbor to under-tip configurations as a function of tunneling current, potential barrier variation with tip height and sample bias, drift rate measurement, a caption for the movie, and discussions about the mechanism of tip−molecule distance dependent variation of occupation probability (PDF)

Evolution of $I-t$ spectra with the variation of tip height (AVI)

■ AUTHOR INFORMATION

Corresponding Authors

*E-mail: hjgao@iphy.ac.cn (H.-J.G.).

*E-mail: sxdu@iphy.ac.cn (S.-X.D.).

DOI: 10.1021/acs.nanolett.8b01019
Nano Lett. 2018, 18, 4704−4709

ORCID

Yun Cao: 0000-0002-7518-2481
Cristian A. Strassert: 0000-0002-1964-0169
Karl-Heinz Ernst: 0000-0002-2077-4922
Shixuan Du: 0000-0001-9323-1307
Hong-Jun Gao: 0000-0002-6766-0623

Author Contributions

The manuscript was written through contributions of all authors. All authors have given approval to the final version of the manuscript.

Notes

The authors declare no competing financial interest.

■ ACKNOWLEDGMENTS

We thank Min Ouyang, Jin-Hai Mao, Yu-Yang Zhang, Geng Li, and Sokrates T. Pantelides for helpful discussions. We acknowledge financial support from the National Natural Science Foundation of China (Nos. 61504149, 21661132006, 61390501, and 61622116), the President Funds of University of Chinese Academy of Sciences, the Transregional Collaborative Research Center TRR 61, and the CAS Key Laboratory of Vacuum Physics.

■ REFERENCES

(1) Schliwa, M.; Woehlke, G. *Nature* **2003**, *422*, 759−765.
(2) Tierney, H. L.; Baber, A. E.; Sykes, E. C. H.; Akimov, A.; Kolomeisky, A. B. *J. Phys. Chem. C* **2009**, *113*, 10913−10920.
(3) Tierney, H. L.; Calderon, C. E.; Baber, A. E.; Sykes, E. C. H.; Wang, F. *J. Phys. Chem. C* **2010**, *114*, 3152−3155.
(4) Shirai, Y.; Osgood, A. J.; Zhao, Y. M.; Kelly, K. F.; Tour, J. M. *Nano Lett.* **2005**, *5*, 2330−2334.
(5) Kudernac, T.; Ruangsupapichat, N.; Parschau, M.; Macia, B.; Katsonis, N.; Harutyunyan, S. R.; Ernst, K.-H.; Feringa, B. L. *Nature* **2011**, *479*, 208−211.
(6) Fletcher, S. P.; Dumur, F.; Pollard, M. M.; Feringa, B. L. *Science* **2005**, *310*, 80−82.
(7) van Delden, R. A.; ter Wiel, M. K. J.; Pollard, M. M.; Vicario, J.; Koumura, N.; Feringa, B. L. *Nature* **2005**, *437*, 1337−1340.
(8) Tierney, H. L.; Murphy, C. J.; Jewell, A. D.; Baber, A. E.; Iski, E. V.; Khodaverdian, H. Y.; McGuire, A. F.; Klebanov, N.; Sykes, E. C. H. *Nat. Nanotechnol.* **2011**, *6*, 625−629.
(9) Perera, U. G. E.; Ample, F.; Kersell, H.; Zhang, Y.; Vives, G.; Echeverria, J.; Grisolia, M.; Rapenne, G.; Joachim, C.; Hla, S. W. *Nat. Nanotechnol.* **2013**, *8*, 46−51.
(10) Kistemaker, J. C. M.; Stacko, P.; Visser, J.; Feringa, B. L. *Nat. Chem.* **2015**, *7*, 890−896.
(11) Chiaravalloti, F.; Gross, L.; Rieder, K.-H.; Stojkovic, S. M.; Gourdon, A.; Joachim, C.; Moresco, F. *Nat. Mater.* **2007**, *6*, 30−33.
(12) Manzano, C.; Soe, W. H.; Wong, H. S.; Ample, F.; Gourdon, A.; Chandrasekhar, N.; Joachim, C. *Nat. Mater.* **2009**, *8*, 576−579.
(13) Gimzewski, J. K.; Joachim, C.; Schlittler, R. R.; Langlais, V.; Tang, H.; Johannsen, I. *Science* **1998**, *281*, 531−533.
(14) Gao, L.; Liu, Q.; Zhang, Y. Y.; Jiang, N.; Zhang, H. G.; Cheng, Z. H.; Qiu, W. F.; Du, S. X.; Liu, Y. Q.; Hofer, W. A.; Gao, H. *J. Phys. Rev. Lett.* **2008**, *101*, 197209.
(15) Zhong, D.; Bloemker, T.; Wedeking, K.; Chi, L.; Erker, G.; Fuchs, H. *Nano Lett.* **2009**, *9*, 4387−4391.
(16) Wang, W.; Shi, X.; Jin, M.; Minot, C.; Van Hove, M. A.; Collin, J.-P.; Lin, N. *ACS Nano* **2010**, *4*, 4929−4935.
(17) Neumann, J.; Gottschalk, K. E.; Astumian, R. D. *ACS Nano* **2012**, *6*, 5242−5248.
(18) Ohmann, R.; Meyer, J.; Nickel, A.; Echeverria, J.; Grisolia, M.; Joachim, C.; Moresco, F.; Cuniberti, G. *ACS Nano* **2015**, *9*, 8394−8400.
(19) Zhang, Y.; Kersell, H.; Stefak, R.; Echeverria, J.; Iancu, V.; Perera, U. G. E.; Li, Y.; Deshpande, A.; Braun, K. F.; Joachim, C.; Rapenne, G.; Hla, S. W. *Nat. Nanotechnol.* **2016**, *11*, 706−713.
(20) Du, S.-x.; Wang, Y.-l.; Liu, Q.; Zhang, H.-g.; Guo, H.-m.; Gao, H.-j. *Front. Phys. China* **2010**, *5*, 380−386.
(21) Yan, S.; Ding, Z.; Xie, N.; Gong, H.; Sun, Q.; Guo, Y.; Shan, X.; Meng, S.; Lu, X. *ACS Nano* **2012**, *6*, 4132−4136.
(22) Kim, H. W.; Han, M.; Shin, H. J.; Lim, S.; Oh, Y.; Tamada, K.; Hara, M.; Kim, Y.; Kawai, M.; Kuk, Y. *Phys. Rev. Lett.* **2011**, *106*, 146101.
(23) Zhang, H.-G.; Mao, J.-H.; Liu, Q.; Jiang, N.; Zhou, H.-T.; Guo, H.-M.; Shi, D.-X.; Gao, *H.-J. Chin. Phys. B* **2010**, *19*, 018105.
(24) Palma, C.-A.; Bjork, J.; Rao, F.; Kuehne, D.; Klappenberger, F.; Barth, J. V. *Nano Lett.* **2014**, *14*, 4461−4468.
(25) Baber, A. E.; Tierney, H. L.; Sykes, E. C. H. *ACS Nano* **2008**, *2*, 2385−2391.
(26) Gehrig, J. C.; Penedo, M.; Parschau, M.; Schwenk, J.; Marioni, M. A.; Hudson, E. W.; Hug, H. *J. Nat. Commun.* **2017**, *8*, 14404.
(27) Grill, L.; Rieder, K. H.; Moresco, F.; Rapenne, G.; Stojkovic, S.; Bouju, X.; Joachim, C. *Nat. Nanotechnol.* **2007**, *2*, 95−98.
(28) Pawlak, R.; Fremy, S.; Kawai, S.; Glatzel, T.; Fang, H.; Fendt, L.-A.; Diederich, F.; Meyer, E. *ACS Nano* **2012**, *6*, 6318−6324.
(29) Metz, J.; Schneider, O.; Hanack, M. *Inorg. Chem.* **1984**, *23*, 1065−1071.
(30) Beck, A.; Mangold, K. M.; Hanack, M. *Chem. Ber.* **1991**, *124*, 2315−2321.
(31) Hanack, M.; Meng, D. Y.; Beck, A.; Sommerauer, M.; Subramanian, L. R. *J. Chem. Soc., Chem. Commun.* **1993**, *0*, 58−60.
(32) Deng, Z. T.; Guo, H. M.; Guo, W.; Gao, L.; Cheng, Z. H.; Shi, D. X.; Gao, H. J. *J. Phys. Chem. C* **2009**, *113*, 11223−11227.
(33) Liu, Q.; Zhang, Y. Y.; Jiang, N.; Zhang, H. G.; Gao, L.; Du, S. X.; Gao, H. *J. Phys. Rev. Lett.* **2010**, *104*, 166101.
(34) Eigler, D. M.; Schweizer, E. K. *Nature* **1990**, *344*, 524−526.
(35) Bohringer, M.; Morgenstern, K.; Schneider, W. D.; Berndt, R. *Angew. Chem., Int. Ed.* **1999**, *38*, 821−823.
(36) Moresco, F. *Single Molecular Machines and Motors* **2015**, 165−186.
(37) Ladenthin, J. N.; Frederiksen, T.; Persson, M.; Sharp, J. C.; Gawinkowski, S.; Waluk, J.; Kumagai, T. *Nat. Chem.* **2016**, *8*, 935−940.
(38) Stroscio, J. A.; Celotta, R. *J. Science* **2004**, *306*, 242−247.
(39) Stipe, B. C.; Rezaei, M. A.; Ho, W. *Science* **1998**, *279*, 1907−1909.
(40) Stroscio, J. A.; Eigler, D. M. *Science* **1991**, *254*, 1319−1326.
(41) Whitman, L. J.; Stroscio, J. A.; Dragoset, R. A.; Celotta, *R. J. Science* **1991**, *251*, 1206−1210.
(42) Jiang, N.; Zhang, Y. Y.; Liu, Q.; Cheng, Z. H.; Deng, Z. T.; Du, S. X.; Gao, H. J.; Beck, M. J.; Pantelides, S. T. *Nano Lett.* **2010**, *10*, 1184−1188.

DOI: 10.1021/acs.nanolett.8b01019
Nano Lett. 2018, 18, 4704−4709